

---

# Query-Kontext: An Unified Multimodal Model for Image Generation and Editing

---

Yuxin Song<sup>1\*</sup>, Wenkai Dong<sup>1\*</sup>, Shizun Wang<sup>2\*</sup>, Qi Zhang<sup>1</sup>, Song Xue<sup>1</sup>,  
 Tao Yuan<sup>1</sup>, Hu Yang<sup>1</sup>, Haocheng Feng<sup>1</sup>, Hang Zhou<sup>1</sup>, Xinyan Xiao<sup>1</sup>, Jingdong Wang<sup>1</sup><sup>✉</sup>  
<sup>1</sup>Baidu VIS    <sup>2</sup>National University of Singapore  
 \* Equal Contribution    ✉ Corresponding Author

## Abstract

Unified Multimodal Models (UMMs) have demonstrated remarkable performance in text-to-image generation (T2I) and editing (TI2I), whether instantiated as assembled unified frameworks which couple powerful vision-language model (VLM) with diffusion-based generator, or as naive Unified Multimodal Models with an early fusion of understanding and generation modalities. We contend that in current unified frameworks, the crucial capability of multimodal generative reasoning which encompasses instruction understanding, grounding, and image referring for identity preservation and faithful reconstruction, is intrinsically entangled with high-fidelity synthesis. In this work, we introduce Query-Kontext, a novel approach that bridges the VLM and diffusion model via a multimodal “*kontext*” composed of semantic cues and coarse-grained image conditions encoded from multimodal inputs. This design delegates the complex ability of multimodal generative reasoning to powerful VLM while reserving diffusion model’s role for high-quality visual synthesis. To achieve this, we propose a three-stage progressive training strategy. First, we connect the VLM to a lightweight diffusion head via multimodal kontext tokens to unleash the VLM’s generative reasoning ability. Second, we scale this head to a large, pre-trained diffusion model to enhance visual detail and realism. Finally, we introduce a low-level image encoder to improve image fidelity and perform instruction tuning on downstream tasks. Furthermore, we build a comprehensive data pipeline integrating real, synthetic, and open-source datasets, covering diverse multimodal reference-to-image scenarios, including image generation, instruction-driven editing, customized generation, and multi-subject composition. Experiments show that our approach matches strong unified baselines and even outperforms task-specific state-of-the-art methods in several cases.

## 1 Introduction

Unified Multimodal Models (UMMs) have recently achieved notable progress in both image generation (T2I) [68, 27, 12, 38, 5, 26, 31, 55, 66, 64, 90] and editing (TI2I) [6, 104, 102, 54, 48, 25, 45, 82, 87]. Two prominent design paradigms have emerged from this work. The first assembled unified framework leverages external diffusion transformers, such as MMDiT [27, 89], which are paired with off-the-shelf vision–language models (VLMs) or large language models (LLMs) to provide semantic conditioning. The second paradigm, naive UMMs, integrate generation and understanding more tightly through mixed-modal early-fusion transformers [110, 26, 75, 20, 85, 76, 57], where autoregressive modules with strong reasoning ability are jointly trained with diffusion modules specialized in visual synthesis.

While these paradigms expand task coverage and streamline deployment, they also entangle multimodal generative reasoning and high-fidelity rendering. Consequently, the unique strengths of VLMs (semantic understanding, grounding, structured reasoning [80, 2, 3, 22, 23, 100, 108, 99])



Figure 1: Showcase of Query-Kontext model on multimodal reference-to-image tasks.

and diffusion models (photorealistic synthesis and detail fidelity [89, 11, 62, 37, 14, 13, 38]) cannot be fully exploited. We identify two sources of this limitation. First, *assembled* unified frameworks typically use a frozen VLM or LLM as a static feature extractor, narrowing the conditioning signal to only high-level semantics for the diffusion generator. Second, *native* UMMs force generative reasoning and visual rendering to be optimized jointly, introducing capacity competition and hindering generalization, particularly when tasks demand both fine-grained edits and strong semantic control. While attempts to mitigate these issues through methods like mixture-of-experts (e.g., LlamaFusion [71]) or mixture-of-transformers (e.g., BAGEL [26]) have been made, they only partially alleviate the tension.

In this work, we propose **Query-Kontext**, an economic ensemble UMM that leverages the multimodal “*kontext*” composed of semantic and coarse image conditions to cleanly decouple the generative reasoning of VLM from the high-fidelity rendering of diffusion model. To realize this separation, we develop a three-stage progressive training strategy. **Stage 1:** Bridge the VLM to a lightweight diffusion head through “*kontext*” tokens. Using parameter-efficient fine-tuning (LoRA) [39], we **unleash** the potential of VLM and steer it toward multimodal generative reasoning skills such as instruction following, spatial grounding, and identity-preserving image referencing. **Stage 2:** **Scale** the lightweight head to a well-trained large diffusion model (roughly  $10\times$  more parameters). We re-align both the text and “*kontext*” tokens from the VLM to the scaled diffusion model by using text-to-image generation and image-reconstruction objectives. **Stage 3:** Introduce a low-level image encoder [1] that injects fine-grained structural and textural cues into the diffusion model while keeping the VLM frozen. This step strengthens identity preservation [101, 83, 93, 72] and reconstruction fidelity in [54, 102, 41, 98] challenging editing scenarios.

In summary, our contributions are:

- We propose **Query-Kontext**, an economic ensemble UMM that decouples multimodal generative reasoning in VLMs from the high-fidelity visual rendering performed by diffusion models.
- We present a three-stage progressive training strategy that progressively aligns the VLM with increasingly capable diffusion generators while amplifying their respective strengths in generative reasoning and visual synthesis.
- We present a deliberate dataset curation scheme to collect real, synthetic, and carefully filtered open-source datasets to cover diverse multimodal reference-to-image scenarios.

## 2 Query-Kontext

In this work, we propose Query-Kontext, a unified multimodal model for image generation and editing that delegates multimodal generative reasoning to the VLM while reserving the diffusion model’s capability for high-quality visual synthesis. In Sec 2.1, we present the architectural design of the Query-Kontext model (Figure 2). In Sec 2.2, we design a three-stage progressive learning strategy and introduce the details of training recipe (Figure 3). In Sec 2.3, we introduce the implementation details of model hyper-parameters and infrastructures.

### 2.1 Architecture

As shown in Figure 2, Query-Kontext comprises four main components: a Multimodal Large Language Model (MLLM), a connector module, a Multimodal Diffusion Transformer (MMDiT), and a low-level image encoder (VAE). The MLLM is initialized with the Qwen2.5-VL model [3], which encodes and fuses multimodal inputs including the text prompt, input image(s), and a set of learnable query tokens. The output is a fixed-length sequence of *kontext* tokens  $Q = \{q_1, \dots, q_K\}$  which serves as coarse image-level conditioning for the diffusion decoder while providing high-level semantic cues. Intuitively, the *kontext* tokens  $Q$  encode what content should appear in the output image (the semantic information from the text prompt) and how the output should incorporate visual cues from the provided input images, as enforced by the training supervision in Sec. 2.2. The *kontext*  $Q$  and text tokens  $T$  are passed through a lightweight connector module to align them with the diffusion model’s latent space. In practice, we concatenate the connector-generated text embeddings with the *kontext* embeddings, thereby enriching the semantic context available to the diffusion model.

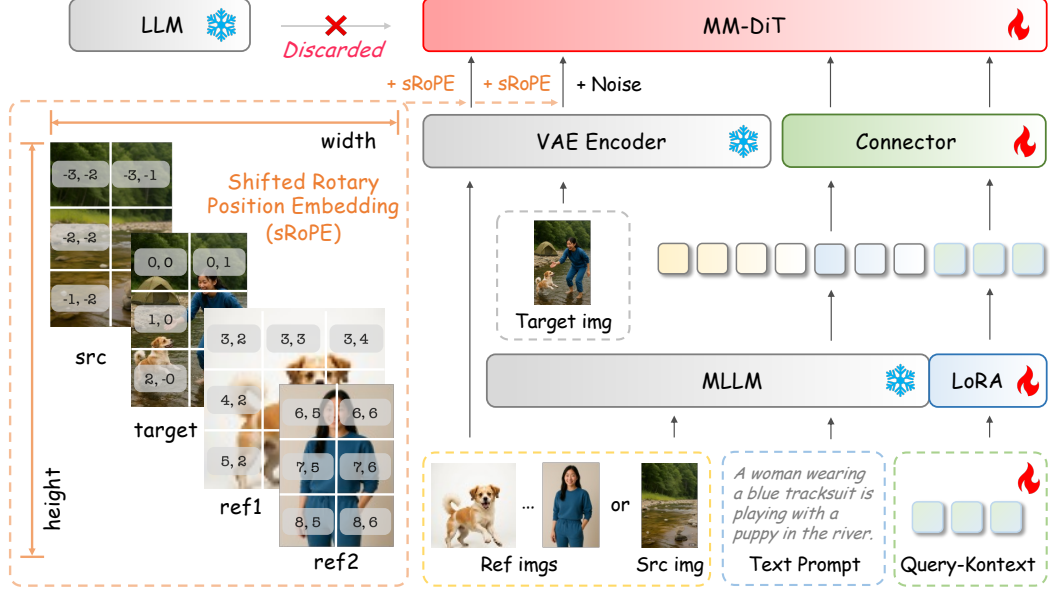


Figure 2: **The overall framework of the unified multi-modal to image generation and editing model, Query-Kontext.**

We initialize the diffusion model using our in-house MMDiT model and replace its original text encoder with the MLLM (*training details for this alignment are discussed in Sec. 2.2*). We concatenate the sequence of text  $T$  and *kontext* tokens  $Q$  from the MLLM with: (i) the noisy image latent at the current diffusion step  $t$ , and (ii) the low-level visual feature tokens extracted from the input image(s) by the VAE. The concatenated sequence is then fed into the MMDiT model in an in-context manner [48, 106], allowing the diffusion model to attend to both the textual prompt and the visual cues from the input images.

Moreover, we distinguish between naive UMMs and assembled UMMs in Table 1. The comparison highlights whether each model trains from scratch, freezes parameters, or adapts pretrained components, and specifies the flow of information through text embeddings (TE), low-level image embeddings (LE), and query embeddings (QE). In particular, query embeddings naturally unleash the in-context learning capabilities of the VLM, enabling the model to reason over multimodal inputs and generate coherent images. Unlike prior methods, **our Query-Kontext integrates query embeddings alongside text and low-level image embeddings, while effectively decoupling understanding and generation modules for improved efficiency and flexibility.**

Furthermore, we design a *shifted 2D Rotary Position Embedding* (RoPE) scheme [73, 93] to incorporate multi-image positional conditioning and avoid confusion among multiple reference images (as illustrated in Figure 2). In the standard diffusion architecture, each spatial position of a latent feature map (with size of  $h \times w$ ) is identified by a 2D index  $(i, j)$ , where  $i \in [0, w - 1]$  and  $j \in [0, h - 1]$ . We introduce a task-specific prior to adjust these coordinates based on the fidelity requirements of the input images. For tasks requiring pixel-level fidelity to an input image (e.g., instruction-based editing), we treat the input image as a *source image*, denoted  $img_{src}$ . For tasks requiring identity preservation (e.g., personalized generation or multi-image composition), we treat the input image as a *reference image*, denoted  $img_{ref}$ . We then shift the coordinate indices of the VAE latent for each image type accordingly: for reference image latents, we shift indices into the positive quadrant, whereas for the source image latent, we shift into the negative quadrant. we define the coordinates for the  $n$ -th reference latent as:

$$(i_{ref}^n, j_{ref}^n) = (i + w * n, j + h * n) \quad (1)$$

where  $i \in [0, w - 1]$ ,  $j \in [0, h - 1]$  and  $n \in [1, N]$ . Meanwhile, for the source image latent we shift the coordinates in the negative direction:

$$(i'_{src}, j'_{src}) = (-i, -j), \quad (2)$$

Method	Module			Information		
	Understanding	Connector	Generation	TE	LE	QE
<b>Native UMMs</b>						
Janus-Pro [20]	🔥	-	🔥	✓	✗	✗
OmniGen2 [92]	❄️ → 🔥	-	🔥	✓	✓	✗
BAGEL [26]	🔥	-	🔥	✓	✗	✗
<b>Assembled UMMs</b>						
Metaquery [66]	❄️	🔥	❄️ → 🔥	✓	✗	✓
Step1X-Edit [54]	❄️	🔥	❄️ → 🔥	✓	✓	✗
Uniworld-v1 [52]	❄️	🔥	❄️ → 🔥	✓	✓	✗
FLUX.1 Kontext [48]	❄️	-	🔥	✓	✓	✗
Qwen-Image [90]	❄️	-	🔥	✓	✓	✗
<b>Query-Kontext (Ours)</b>	❄️ → 🔥	🔥	❄️ → 🔥	✓	✓	✓

Table 1: **Comparison of mainstream unified multimodal models on the modeling paradigms and the information flow.** 🔥 denotes training from scratch, ❄️ indicates freezing the parameters during training and ❄️ → 🔥 represents training from a pretrained model. For the input modalities, “TE” refers to text embeddings, “LE” to low-level image embeddings, and “QE” to query embeddings.

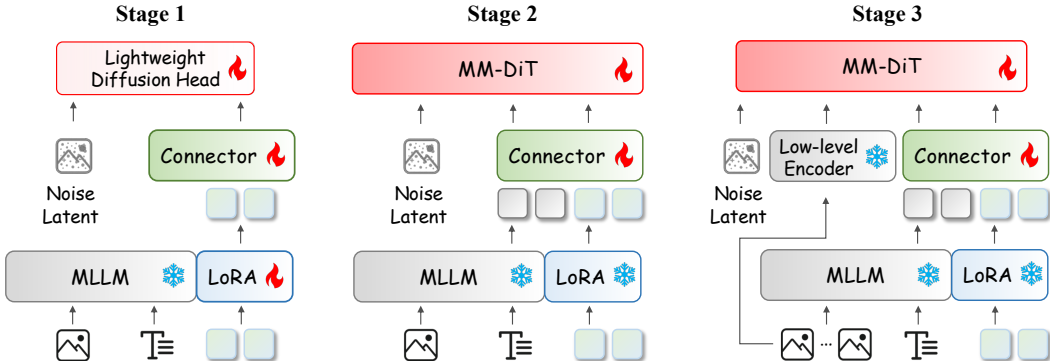


Figure 3: **Three training stages of Query-Kontext.** Note that the Diffusion Head is only used in the Stage 1. In the Stage 2 and 3, we scale up Diffusion model to 10x parameters and keep MLLM frozen to provide coarse-grained image conditions.

where  $i \in [0, w - 1]$ ,  $j \in [0, h - 1]$  and  $n \in [1, N]$ . Finally, we add the shifted RoPE on the feature maps of the input image latent(s) and the noisy latent at their respective shifted coordinates (i.e., added element-wise to each spatial location).

## 2.2 Individualized-Teaching Curriculum

As shown in Figure 3, we propose a three-stage progressive training strategy that both unlocks the generative reasoning capabilities of the VLM and progressively aligns it with increasingly powerful diffusion generators. As a result, Query-Kontext, guided by multimodal *kontext* tokens, effectively decouples the multimodal generative reasoning of the VLM from the high-fidelity visual rendering carried out by diffusion models.

**Stage 1:** We unleash the generative reasoning potential of the MLLM through two key architectural designs: we first use learnable query tokens (“kontext”) to represent a mixture of semantic cues and coarse-grained image conditions, and then align the output *kontext* tokens with a lightweight diffusion head that performs noisy prediction at a coarse level. We train all parameters of the connector, the diffusion head, and the MLLM’s LoRA modules on a trio of tasks: text-to-image generation, image reconstruction, and image transformation (see Section 3). This training methodology preserves the

Table 2: Configuration of Query-Kontext architecture.

Configuration	MLLM		VAE		Connector	MMDiT
	ViT	LLM	Enc	Dec		
# Layers	32	28	8	14	2	42
# Num Heads (Q / KV)	16 / 16	28 / 4	-	-	-	40 / 40
Head Size	80	128	-	-	-	64
Intermediate Size	3,456	18,944	-	-	-	10240
Patch / Scale Factor	14	-	8x8	8x8	-	2
Channel Size	-	-	16	16	-	-
# Parameters	7B		34M	50M	5.9M	10B

MLLM’s inherent language-vision understanding while cultivating its emergent ability for multimodal generative reasoning.

**Stage 2:** Next, we replace the lightweight diffusion head with our in-house diffusion model based on the MMDiT architecture for high-fidelity generation. In Stage 2, the full MLLM parameters (the LoRA parameters are merged into the MLLM) remain frozen, and we optimize the *kontext* tokens, the connector, and all parameters of the large diffusion model. In preliminary experiments, we observed that completely freezing the diffusion model was feasible for smaller head but failed for a larger diffusion model (*the experiments details and discussion are available in Section 6*). Therefore, we allow the diffusion model to be full-parameters fine-tuning in this stage. To keep training efficient, Query-Kontext is trained only on text-to-image generation and image reconstruction tasks in this stage, which accelerates convergence and reduces training cost for fast alignment from MLLM to the diffusion model.

**Stage 3:** Finally, we introduce a dedicated low-level image encoder for source or reference images to further refine the diffusion model for high-fidelity image referring. In Stage 3, the MLLM remains fully frozen, and we optimize only the Query-Kontext tokens and the connector. Additionally, we apply the LoRA-based fine-tuning to the diffusion model itself to preserve its high-quality image synthesis ability while extending it to all our tasks. This includes not only standard text-to-image generation but also instruction-guided image editing, user-customized image generation, and multi-subject composition tasks.

### 2.3 Implementation

**Architecture.** We initialize the MLLM from Qwen2.5-VL-7B and implement the connector as a two-layer MLP. (*details of architecture configuration are provided in Table 2.*) The connector maps text and kontext tokens into the diffusion latent space; the outputs are concatenated before being fed to the diffusion transformer. Moreover, we implement the diffusion head in the stage a with a lightweight MMDiT architecture ( $\sim 870M$  parameters). We set the max reference images  $N = 2$  and  $K = 128$  in Query-kontext  $Q = \{q_1, \dots, q_K\}$ . We set rank  $r_d = 256$ ,  $\alpha_d = 256$  in the diffusion model’s and rank  $r_m = 128$ ,  $\alpha_m = 256$  in the MLLM’s LoRA.

**Training recipe.** The default configuration on the resolution with  $512 \times 512$  is provided in Table 3. After Stage 3, we introduce a resolution upscaling stage using the same mixed multi-task dataset at a higher resolution. In this stage, the training resolution is increased to  $1024 \times 1024$ , the learning rate is further reduced to  $1 \times 10^{-5}$ , and training continues for an additional 3,000 steps with a global batch size of 256.

**Infrastructure.** We adopt a hybrid parallel optimization strategy during training. we enable tensor parallelism on the VLM side. For the diffusion model, we use parameter sharding (ZeRO Stage-2) together with bfloat16 (BF16) mixed-precision training. To keep sequence lengths uniform within a mini-batch, we maintain two independent bucketeers—by image aspect ratio (supporting 1:1, 1:2, 2:3, 3:4, 3:5, 4:5, and 9:16) and by the number of reference images—so that samples in the same batch produce the same number of latent tokens, reducing padding and improving throughput.

Table 3: **The data outline and training details about each training stage.** Where,  $Q.$  denotes the Query-kontext tokens,  $Con.$  is Connector module.

Stage	Stage 1	Stage 2	Stage 3
Task	Image Generation Image Reconstruction Image Transformation	Image Generation Image Reconstruction	Instruction Editing Customized Generation Multi-subject
Type	T2I, I2I, TI2I	T2I, I2I	T2I, TI2I
Training Param.	MLLM’s LoRA, $Con.$ , Diffusion head, $Q.$	$Con.$ , MMDiT, $Q.$	MMDiT’s LoRA, $Con.$ , $Q.$
Global Batch Size	512	1024	512
Steps (K)	72	420	30
Learning Rate	1e-4	1e-4	2e-5

### 3 Data Curation

Table 4: **The data outline about each training stage.**  $\dagger$  denotes only the Chinese prompt.

Stage	Task	Data source	Size
1, 2, 3	Image generation, Image reconstruction	ShareGPT-4o-Image[15], BLIP3o[10] in-house real data $\dagger$	30M 170M
1	Image transformation	mmc4[111], OmniCorpus[50]	800K
3	Instruction editing	NHR-Edit[45], GPT-Edit[90], OmniEdit[87] in-house video data in-house real data	3M 2M 300K
	Customized generation	subject200k[74] in-house real data	200K 1.8M
	Multi-subject composition	MUSAR-Gen[34] G4o synthesis data	29K 40K

We constructed a multimodal reference-to-image dataset (as summarized in Table 4) comprising a mixture of real, synthetic, and carefully curated open-source datasets. This dataset spans five categories of tasks: text-to-image generation, image transformation, instruction editing, customized generation, and multi-subject composition.

**Text-to-Image Generation and Image Reconstruction.** We collected 30M open-source English image-text pairs (including ShareGPT-4o-Image [15], BLIP-3o [10], among others) as well as 170M in-house Chinese image-text pairs for text-to-image generation and image reconstruction tasks. The in-house data underwent extensive quality filtering based on image resolution, clarity, aesthetic score, watermark detection, and safety compliance. Among these Chinese data, 150M belong to general categories (balanced across diverse domains), and 20M come from specific vertical domains (e.g., artistic styles, logos, automobiles, text-containing images, celebrities, posters, etc.).

**Image Transformation.** Following the MetaQuery [66], we constructed naturally occurring image pairs from web corpora [17, 50] and generated corresponding open-ended transformation instructions by leveraging multi-modal large language models (MLLMs). Specifically, we clustered images that share the same accompanying caption from sources like MMC4-core[17], OmniCorpus-CC [50] and OmniCorpus-CW [50] by using SigLIP [77] image features, then filtered these clusters by a similarity threshold to obtain 0.8M image transformation triplets. As shown in Figure 4, each triplet contains a source image, an open-ended transformation instruction which is generated by Qwen2.5-VL as shown in Figure 5, and a target image. The instructions cover viewpoint changes (e.g., zoom-in/out, rotation), appearance modifications (e.g., color/material replacement), and structural adjustments (e.g., adding/removing objects).



Figure 4: Examples of the image transformation task. Each row shows a transformation instruction, the source image and the resulting target image, in order from left to right.

**Instruction Editing.** For the image editing instruction task, we first aggregated approximately 3M image-instruction-image triplets from open-source datasets, including NHR-Edit [45](358k samples), GPT-Image-Edit [65](1.5M samples), MagicBrush [43](10k samples), and OmniEdit [87](1.2M samples). We further filtered the MagicBrush subset using CLIP-based image and text similarity scores, and translated all datasets’ instructions into Chinese using a large language model.

Building upon the methodologies of [45, 87, 54], we then constructed a synthetic data pipeline tailored for native Chinese instruction editing, producing an additional 300k high-quality triplets. As illustrated in Figure 6. Given a source image, its segmentation mask, and a caption, we first extract object-level queries (e.g., “man”) and generate diverse editing instructions. Specifically, large language models (Qwen2-72B) generate textual editing prompts from captions, while multimodal models (Qwen2VL-72B) leverage both captions and images to produce more fine-grained attribute modification instructions. In addition, we incorporate template-based instructions (e.g., “remove xxx from the image”) to further handle object remove task. The generated instructions are categorized into four task types: object replacement, object addition, object removal, and attribute modification. Each task is then handled by specialized synthesis models: RF-Solver-Edit-12B [79] or FLUX-Kontext [48] for replacement and attribute edits, mask-based inpainting model [5] for addition and removal, and commercial APIs (e.g., G4o/SeedEdit-v3) for more complex operations. Finally, the generated triplets are filtered through an automatic evaluation stage using Qwen2.5VL-72B, which scores instruction fidelity and image quality, followed by manual verification to ensure reliability. Finally, manual reverse instruction generation is applied by treating the source image as the target, ensuring supervision from authentic images without model-induced artifacts. Moreover, when applying mask-inpainting models to remove large objects, we adopt a mask augmentation strategy to mitigate the influence of shape-guided masks. Figure 7 presents a comparison between results with and without mask augmentation.

Finally, inspired by UniReal [19], we extended our dataset with video-based clusters derived from raw videos to cover more non-rigid editing tasks (e.g., motion changes, viewpoint shifts, view transitions such as zoom-in and zoom-out. Representative data examples are provided in Figure 8.

Qwen2.5-VL Prompt

The first image is the source image, the second image is the target image. create an interesting text prompt that can be used with the source images to generate the target image.

This prompt should include: - one general and unspecific similarity shared with the source image. - all differences that only the target image has. This prompt should NOT include: - any specific details that would allow generating the target image independently without referencing the source image. Remember the prompt should be concise and short (no more than 64 words).

The difference should include but not limited to: Change in Angle. Describe the specific new angle, e.g.: \* Side view, back view, viewed from the front side \* With a closer view, focus on the top of the item \* Cropped in the center, in a horizontal/vertical view

Same Subject, Altered Elements. Specify added/removed elements, e.g.: \* The same jacket but with a person wearing it \* Without the package \* with a bowl on the right \* Show the engine of the same car

Color Change. Describe the new color(s), e.g.: \* Blue and purple flowers instead of yellow \* Turn the color of the vase to cyan \* Same design but in white

Position Change. Specify the new position, e.g.: \* Put the item in the middle \* Move it to the side with a closer view

Background Change. Describe the modified background, e.g.: \* With a clean background \* The daylight turns dim \* Without a background

Quantity Change. State the updated quantity, e.g.: \* Show three trains of the same type

State/Process Change. Describe the transformation or action, e.g.: \* The beef is cooked \* The man is pouring batter into a pan \* Put it down

Here are some of the example: 1. Prompt: The complete front view of the same jersey top. 2. Prompt: Show three blue pot with same floral design, now placed in a cozy dining scene with food, drinks, and side dishes around it. 3. Prompt: The same pair of silver rings captured in another angle with brighter lighting and a clean white background and softer shadows.

Please generate one English prompt and one Chinese prompt, following the JSON format: ['English prompt here', 'Chinese prompt here'].]

Figure 5: Example of the prompt used in Qwen2.5-VL to generate open-ended transformation instructions.

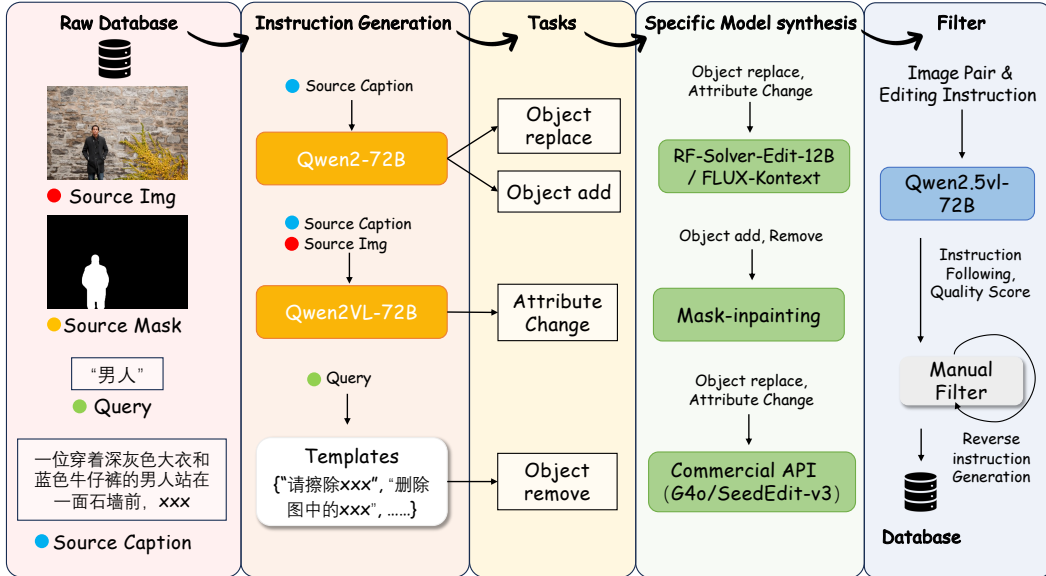


Figure 6: Examples of synthetic data pipeline for instruction Editing.

**Customized Generation.** We leveraged the open-source Subject-200K [74] and UNO-1M [93] datasets for customized (subject-driven) image generation. In addition, we augmented our data with portrait reference triplets synthesized using a dedicated model<sup>1</sup>, which generates reference images of

<sup>1</sup><https://console.bce.baidu.com/qianfan/modelcenter/model/buildIn/detail/am-t3uhhjzbys6w>



Figure 7: Examples of image inpainting with mask augmentation.

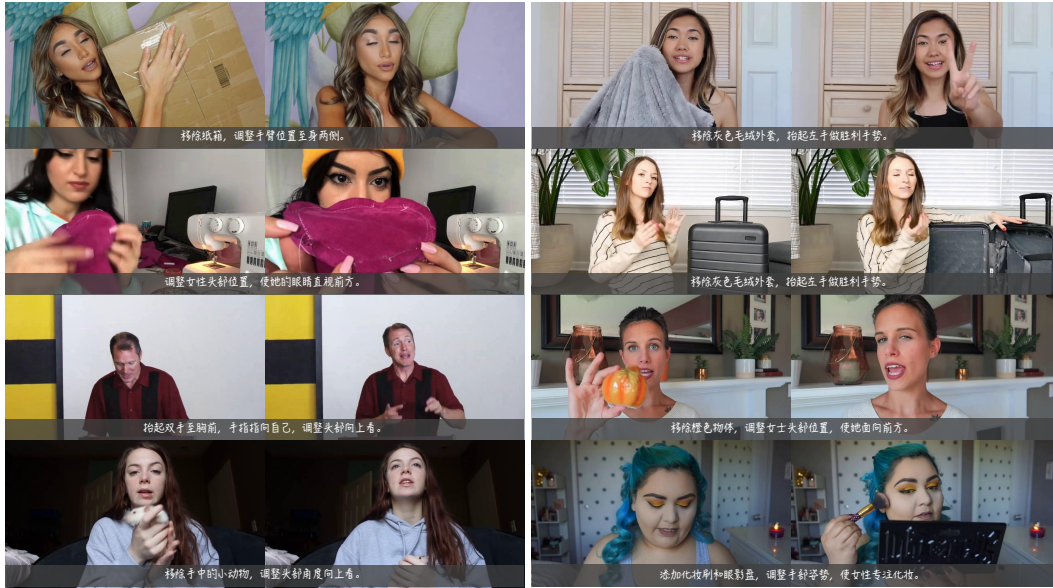


Figure 8: Examples of instruction editing data pair constructed from real video.

specific individuals. Through this approach, we accumulated approximately 0.3M portrait reference

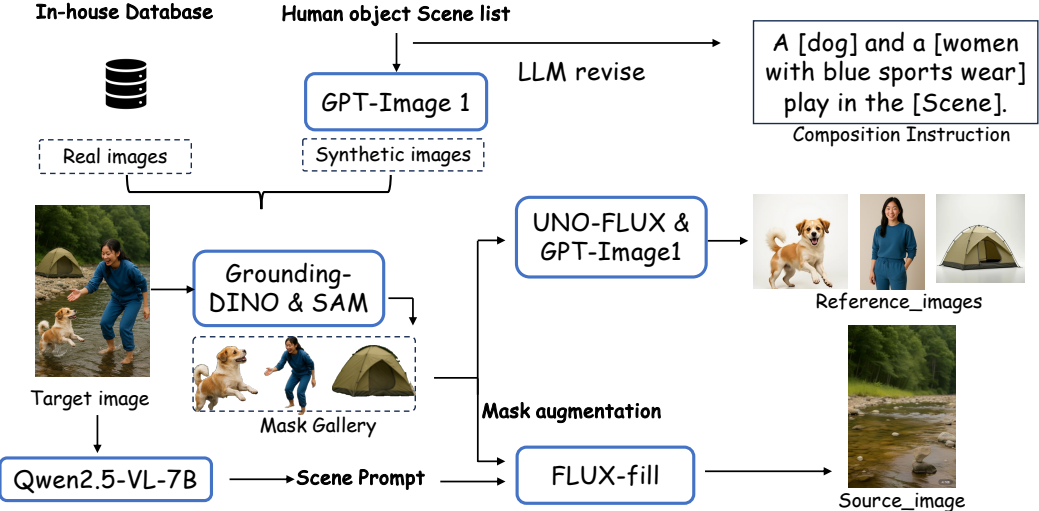


Figure 9: Examples of synthetic data pipeline for Multi-Subject Composition.

samples that maintain high facial similarity to the source subjects while exhibiting substantial diversity in poses, attire, and other attributes.

**Multi-Subject Composition.** Finally, we addressed multi-subject image composition using the open-source MUSAR-Gen [34] dataset and a new synthetic data pipeline. As illustrated in Figure 9, we design a synthetic pipeline to construct high-quality multi-subject composition data. Starting from an in-house database, we combine both real and synthetic images, and generate human–object–scene lists that are further refined by large language models (LLMs) to produce natural composition instructions. Grounding-DINO [53] and SAM [44] are employed to extract object-level masks and build a mask gallery, which provides structural guidance for subsequent composition. Reference images of subjects and objects are synthesized by UNO-FLUX and GPT-Image1, while scene backgrounds are generated by mask-inpainting model. The resulting target images, together with corresponding composition instructions and scene prompts, form diverse training triplets that enhance the coverage of multi-subject scenarios. This yielded 40k multi-subject reference examples, each featuring compositions of multiple humans, objects, and complex scenes, thereby enriching the dataset’s coverage of realistic multi-entity interactions.

## 4 Experiments

### 4.1 Quantitative results

We evaluate Query-Kontext on a comprehensive suite of benchmarks, spanning text-to-image generation, instruction-guided editing, subject-driven customization, and multi-subject composition. Specifically, we report results on GenEval, GEdit-Bench, DreamBooth, and DreamBench.

On GenEval, Query-Kontext attains an overall score of 0.88, matching the SOTA result of unified UMM (BAGEL [26]), as illustrated in Table 5. Our results are reported based on Chinese prompts rewritten by DeepSeek <sup>2</sup>. On GEdit-Bench, Query-Kontext achieves the highest overall performance in instruction-guided editing, with scores of 7.66 on the English split and 7.65 on the Chinese split. These results surpass Qwen-Image (7.56 / 7.52) and GPT-Image (7.53 / 7.30), as shown in Table 6. We note that the Perceptual Quality score exhibits some shortcomings, primarily due to the lack of a reinforcement learning or supervised fine-tuning stage designed to enhance generation quality or photorealism. We leave this exploration in future work. For subject-driven generation on DreamBooth, Query-Kontext establishes new state-of-the-art results with DINO 0.786 and CLIP-I 0.858, significantly outperforming Metaquery (0.737 / 0.851) and UNO-FLUX (0.760 / 0.835), though with a slightly lower CLIP-T (0.307 vs. OmniGen’s 0.315), as shown in Table 7. In Table 8,

<sup>2</sup><https://chat.deepseek.com/>

Table 5: **Quantitative Evaluation results on GenEval [33].**  $\dagger$  refer to the methods using the LLM rewriter.

Model	Single Object	Two Object	Counting	Colors	Position	Attribute Binding	Overall $\uparrow$
Show-o [96]	0.95	0.52	0.49	0.82	0.11	0.28	0.53
Emu3-Gen [86]	0.98	0.71	0.34	0.81	0.17	0.21	0.54
PixArt- $\alpha$ [14]	0.98	0.50	0.44	0.80	0.08	0.07	0.48
SD3 Medium [28]	0.98	0.74	0.63	0.67	0.34	0.36	0.62
FLUX.1 [Dev] [5]	0.98	0.81	0.74	0.79	0.22	0.45	0.66
SD3.5 Large [28]	0.98	0.89	0.73	0.83	0.34	0.47	0.71
JanusFlow [58]	0.97	0.59	0.45	0.83	0.53	0.42	0.63
Lumina-Image 2.0 [69]	-	0.87	0.67	-	-	0.62	0.73
Janus-Pro-7B $\dagger$ [21]	0.99	0.89	0.59	0.90	0.79	0.66	0.80
HiDream-II-Full $\dagger$ [8]	<b>1.00</b>	0.98	0.79	0.91	0.60	0.72	0.83
GPT-Image $\dagger$ [65]	0.99	0.92	0.85	0.92	0.75	0.61	0.84
Seedream 3.0 $\dagger$ [31]	0.99	<b>0.96</b>	<b>0.91</b>	0.93	0.47	0.80	0.84
Qwen-Image $\dagger$ [90]	0.99	0.92	0.89	0.88	0.76	0.77	0.87
BAGEL $\dagger$ [26]	0.98	0.95	0.84	<b>0.95</b>	0.78	0.77	<b>0.88</b>
<b>Query-Kontext<math>\dagger</math></b>	0.98	0.94	0.81	0.91	<b>0.85</b>	<b>0.79</b>	<b>0.88</b>

Table 6: **Quantitative Evaluation results on GEdit-Bench.** G\_SC is Semantic Consistency, G\_PQ is Perceptual Quality, and G\_O is Overall Score which is computed as the geometric mean of G\_SC and G\_PQ, averaged over all samples. All metrics are evaluated by GPT-4. We highlight the **best** and second-best values for each metric.

Model	GEdit-Bench-EN (Full set) $\uparrow$			GEdit-Bench-CN (Full set) $\uparrow$		
	G_SC	G_PQ	G_O	G_SC	G_PQ	G_O
Instruct-Pix2Pix [6]	3.58	5.49	3.68	-	-	-
AnyEdit [103]	3.18	5.82	3.21	-	-	-
MagicBrush [104]	4.68	5.66	4.52	-	-	-
UniWorld-v1 [52]	4.93	7.43	4.85	-	-	-
OmniGen [95]	5.96	5.89	5.06	-	-	-
OmniGen2 [92]	7.16	6.77	6.41	-	-	-
Gemini 2.0 [25]	6.73	6.61	6.32	5.43	6.78	5.36
BAGEL [26]	7.36	6.83	6.52	7.34	6.85	6.50
FLUX.1 Kontext [Pro] [48]	7.02	7.60	6.56	1.11	7.36	1.23
Step1X-Edit [55]	7.66	7.35	6.97	7.20	6.87	6.86
GPT Image 1 [High] [65]	7.85	<u>7.62</u>	7.53	7.67	<u>7.56</u>	7.30
Qwen-Image [90]	8.00	<b>7.86</b>	<u>7.56</u>	7.82	<b>7.79</b>	<u>7.52</u>
<b>Query-Kontext</b>	<b>8.36</b>	7.37	<b>7.66</b>	<b>8.39</b>	7.35	<b>7.65</b>

Query-Kontext achieves the best CLIP-T score (0.336) alongside competitive DINO (0.532) and CLIP-I results (0.731), on the multi-subject composition benchmark DreamBench.

## 4.2 Qualitative Results

We also provide qualitative comparisons across all task categories, including text-to-image generation, instruction editing, and customized generation, under both Chinese and English prompts. Representative examples are shown in Figure 1.

## 4.3 Shifted RoPE

We further examine the effect of the proposed shifted 2D-RoPE mechanism for handling reference images. With *source* input images, the model tends to preserve the pixel-level fidelity of the input, producing faithful reconstructions. In contrast, with *reference* input images, the model emphasizes

Table 7: **Quantitative results for single-subject driven generation on Dreambooth.** We highlight the **best** and second-best values.

Method	DINO $\uparrow$	CLIP-I $\uparrow$	CLIP-T $\uparrow$
<i>Tuning-free</i>			
Textual Inversion [30]	0.569	0.780	0.255
DreamBooth [70]	0.668	0.803	0.305
BLIP-Diffusion [49]	0.670	0.805	0.302
<i>Specialist Models</i>			
ELITE [88]	0.647	0.772	0.296
Re-Imagen [18]	0.600	0.740	0.270
OminiControl [74]	0.684	0.799	0.312
FLUX.1 IP-Adapter [5]	0.582	0.820	0.288
UNO-FLUX [93]	<u>0.760</u>	0.835	0.304
<i>Generalist Models</i>			
OmniGen [94]	0.693	0.801	<b>0.315</b>
Metaquery [66]	0.737	<u>0.851</u>	0.301
<b>Query-Kontext</b>	<b>0.786</b>	<b>0.858</b>	<u>0.307</u>

Table 8: **Quantitative results for multi-subject driven generation on Dreambench.** We highlight the **best** and second-best values for each metric.

Method	DINO $\uparrow$	CLIP-I $\uparrow$	CLIP-T $\uparrow$
<i>Tuning-free</i>			
DreamBooth [70]	0.430	0.695	0.308
BLIP-Diffusion [49]	0.464	0.698	0.300
<i>Specialist Models</i>			
Subject Diffusion [56]	0.506	0.696	0.310
MIP-Adapter [40]	0.482	0.726	0.311
MS-Diffusion [84]	0.525	0.726	0.319
UNO-FLUX [93]	<b>0.542</b>	<b>0.733</b>	0.322
<i>Generalist Models</i>			
OmniGen [94]	0.511	0.722	<u>0.331</u>
<b>Query-Kontext</b>	<u>0.532</u>	<u>0.731</u>	<b>0.336</b>

instruction following and generalization, maintaining subject identity while generating more diverse outputs. Comparative results on the DreamBooth benchmark using source versus reference images are reported in Table 9.

#### 4.4 Query-Kontext Convergence

In Stage 2, we analyze the convergence behavior of the diffusion model when conditioned on two settings: (i) text-only embeddings from an LLM and (ii) the mixed conditioning from both text tokens and Query-Kontext tokens generated by our fine-tuned VLM. We observe that replacing the LLM with our VLM leads to faster alignment of the diffusion model and produces superior visual results compared to the LLM-conditioned baseline, as shown in Figure 10. This demonstrates that decoupling multimodal reasoning from visual generation via Query-Kontext not only accelerates convergence but also unleashes the full potential of both the VLM and the diffusion model.

#### 4.5 LoRA Rank

We evaluate LoRA ranks  $\{64, 128, 256\}$  on both the diffusion model and the MLLM adapters, observing faster convergence at higher ranks with marginal quality gains beyond  $r=128$ .

Table 9: The comparison between the shifted RoPE on *source* or *reference* image.

Method	DINO $\uparrow$	CLIP-I $\uparrow$	CLIP-T $\uparrow$
w/ $img_{src}$	0.865	0.914	0.289
w/ $img_{ref}$	0.786	0.858	0.307

Table 10: Ablations on positional encoding, number of reference images, and LoRA ranks.

Setting	DINO	CLIP-I	CLIP-T
LoRA $r=64$	0.752	0.841	0.298
LoRA $r=128$	0.786	0.858	0.307
LoRA $r=256$	0.777	0.834	0.311

## 5 Related Work

### 5.1 Instruction-based Image Editing

Early diffusion-based editing splits into *training-free* and *training-based* approaches. Training-free methods manipulate the denoising trajectory via inversion [60, 61, 43, 24, 78, 16] or attention control [9, 36, 67] and require no additional training, but often struggle with fine-grained instruction fidelity and identity preservation. InstructPix2Pix [6] pioneered training-based approaches [16, 109, 51, 103, 107] by finetuning a pretrained diffusion backbone on curated (image, instruction, edited-image) triplets, yielding stronger instruction following and higher fidelity. More recently, a trend towards tighter integration of *multimodal* understanding and generation has emerged to empower more complex editing instructions. Works like SmartEdit [41] and Step1X-Edit [55] leverage MLLM latent representations to guide structured or latent-conditioned editing, ACE [35], ACE++ [59] and FLUX.1 Kontext [48] integrate text and image context for instruction-guided editing. UniVG [29], SeedEdit 3.0 [82], and Qwen-Image [90] demonstrate generalist architectures capable of diverse tasks while preserving identity and fidelity.

### 5.2 Unified Multimodal Models

Unified Multimodal Models (UMMs) have recently attracted significant attention for their ability to unify both understanding and generation within a single architecture. Existing approaches can be broadly categorized into two strategies. The first strategy develops *native* UMMs [75, 110, 96, 97, 91, 20, 57, 85, 76, 26], which are trained to fuse multimodal understanding and generation capabilities at the early stage, usually involving autoregressive or diffusion modeling. While conceptually elegant, they often present considerable challenges in training and scaling. The second strategy *assembles* unified frameworks [66, 90, 10, 48, 54, 19, 29, 17] by coupling existing vision-language models (VLMs)[3, 81] for understanding with powerful diffusion-based generators[27, 89, 47]. This is typically achieved through learnable tokens or tuning adapters. Our work builds on this line of research, introducing a more refined mechanism for cross-modal representation fusion and controllable generation.

### 5.3 Editing Data Curation

High-quality and diverse datasets of  $\langle$ original image, instruction, edited image $\rangle$  triplets are fundamental for training powerful editing models. MagicBrush [104] represents the manual annotation approach. InstructPix2Pix [6] pioneered data synthesis by using GPT-3 [7] and Prompt-to-Prompt [36]. To improve quality, HIVE [105] introduced human feedback for quality assessment and training. HQ-Edit [42] and UltraEdit [109] scaled up dataset size and difficulty using more powerful models like GPT-4V [63] and DALL-E 3 [4], along with fine-grained annotations. SEED-Data-Edit [32] enhances diversity through re-generation and re-annotation techniques, while SeedEdit 3.0 [82] systematically upgrades both data sources and data merging. More recently, NHR-Edit [46] automates

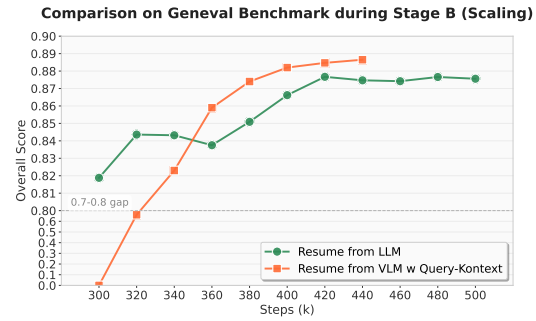


Figure 10: **Convergence validation of Query-Kontext.** Comparison on our in-house MMDiT between VLM re-alignment with Query-Kontext and LLM-based resumption.

the mining of high-quality triplets from powerful open-sourced generative models like FLUX [47], reducing manual effort and improving data realism.

## 6 Discussion

**Economical Alignment between VLM and Diffusion Model.** Query-Kontext builds on a powerful VLM and an MMDiT-based diffusion model, leveraging the strengths of each to construct a unified multimodal-to-image generation system. The training process was conducted on 192 NVIDIA H100 GPUs (80GB), which amounts to roughly 10% of the computational resources typically required to train a large-scale diffusion model from scratch (e.g., Qwen-Image) or an integrated multimodal transformer (e.g., BAGEL). This economical alignment allows us to allocate resources more effectively, focusing on higher-level and underexplored post-training tasks such as multi-subject composition, multi-image generation, and interleaved text–image generation.

**Scaling of the Diffusion Model.** By decoupling multimodal generative reasoning in the VLM from high-fidelity visual synthesis in the diffusion model, our framework enables independent exploration on the scaling laws of each component. This separation is crucial, as VLMs and diffusion models often exhibit competing capacity requirements and benefit from different parameter budgets. In Stage 2, we attempted alignment with in-house diffusion backbones of varying sizes (0.9B, 4B, and 10B parameters). However, alignment was not always successful, particularly when employing a lightweight connector to bridge a heavy and frozen diffusion model (e.g., 10B parameters). To mitigate this issue, we unfroze the diffusion model parameters during Stage 2 training, thereby avoiding an intensive grid search over connector hyperparameters. Investigating the scaling laws governing the connector remains an important direction for future work.

## 7 Conclusion

In this work, we introduced Query-Kontext, an economical unified multimodal-to-image framework that decouples multimodal generative reasoning (handled by the VLM) from high-fidelity rendering (handled by the diffusion model). To fully harness the potential of both components, we proposed a three-stage progressive training strategy that progressively aligns the VLM with increasingly capable diffusion generators while amplifying their complementary strengths. In addition, we curated a multimodal reference-to-image dataset mixture spanning real, synthetic, and carefully filtered open-source data. Extensive experiments demonstrate that our framework achieves competitive performance across diverse tasks, including image generation, instruction editing, customized subject synthesis, and multi-subject composition.

## References

- [1] Stability AI. sd-vae-ft-ema, 2024. URL <https://huggingface.co/stabilityai/sd-vae-ft-ema>.
- [2] Jinze Bai, Shuai Bai, Shusheng Yang, Shijie Wang, Sinan Tan, Peng Wang, Junyang Lin, Chang Zhou, and Jingren Zhou. Qwen-vl: A frontier large vision-language model with versatile abilities. *arXiv:2308.12966*, 2023.
- [3] Shuai Bai, Keqin Chen, Xuejing Liu, Jialin Wang, Wenbin Ge, Sibo Song, Kai Dang, Peng Wang, Shijie Wang, Jun Tang, Humen Zhong, Yuanzhi Zhu, Mingkun Yang, Zhaohai Li, Jianqiang Wan, Pengfei Wang, Wei Ding, Zheren Fu, Yiheng Xu, Jiabo Ye, Xi Zhang, Tianbao Xie, Zesen Cheng, Hang Zhang, Zhibo Yang, Haiyang Xu, and Junyang Lin. Qwen2.5-vl technical report. *arXiv preprint arXiv:2502.13923*, 2025.
- [4] James Betker, Gabriel Goh, Li Jing, Tim Brooks, Jianfeng Wang, Linjie Li, Long Ouyang, Juntang Zhuang, Joyce Lee, Yufei Guo, et al. Improving image generation with better captions. *OpenAI blog*, 2023.
- [5] BlackForest. Flux. <https://github.com/black-forest-labs/flux>, 2024.
- [6] Tim Brooks, Aleksander Holynski, and Alexei A Efros. Instructpix2pix: Learning to follow image editing instructions. In *Proceedings of the IEEE/CVF conference on computer vision and pattern recognition*, pages 18392–18402, 2023.
- [7] Tom Brown, Benjamin Mann, Nick Ryder, Melanie Subbiah, Jared D Kaplan, Prafulla Dhariwal, Arvind Neelakantan, Pranav Shyam, Girish Sastry, Amanda Askell, et al. Language models are few-shot learners. In *NeurIPS*, 2020.
- [8] Qi Cai, Jingwen Chen, Yang Chen, Yehao Li, Fuchen Long, Yingwei Pan, Zhaofan Qiu, Yiheng Zhang, Fengbin Gao, Peihan Xu, et al. Hidream-i1: A high-efficient image generative foundation model with sparse diffusion transformer. *arXiv preprint arXiv:2505.22705*, 2025.
- [9] Mingdeng Cao, Xintao Wang, Zhongang Qi, Ying Shan, Xiaohu Qie, and Yinqiang Zheng. Masactr: Tuning-free mutual self-attention control for consistent image synthesis and editing. In *Proceedings of the IEEE/CVF international conference on computer vision*, pages 22560–22570, 2023.
- [10] Juhai Chen, Zhiyang Xu, Xichen Pan, Yushi Hu, Can Qin, Tom Goldstein, Lifu Huang, Tianyi Zhou, Saining Xie, Silvio Savarese, et al. Blip3-o: A family of fully open unified multimodal models-architecture, training and dataset. *arXiv preprint arXiv:2505.09568*, 2025.
- [11] Junsong Chen, Jincheng Yu, Chongjian Ge, Lewei Yao, Enze Xie, Yue Wu, Zhongdao Wang, James Kwok, Ping Luo, Huchuan Lu, et al. Pixart-alpha: Fast training of diffusion transformer for photorealistic text-to-image synthesis. *arXiv preprint arXiv:2310.00426*, 2023.
- [12] Junsong Chen, Chongjian Ge, Enze Xie, Yue Wu, Lewei Yao, Xiaozhe Ren, Zhongdao Wang, Ping Luo, Huchuan Lu, and Zhenguo Li. Pixart-sigma: Weak-to-strong training of diffusion transformer for 4k text-to-image generation. In *ECCV*, 2024.
- [13] Junsong Chen, Chongjian Ge, Enze Xie, Yue Wu, Lewei Yao, Xiaozhe Ren, Zhongdao Wang, Ping Luo, Huchuan Lu, and Zhenguo Li. Pixart- $\sigma$ : Weak-to-strong training of diffusion transformer for 4k text-to-image generation. In *European Conference on Computer Vision*, pages 74–91. Springer, 2024.
- [14] Junsong Chen, Jincheng Yu, Chongjian Ge, Lewei Yao, Enze Xie, Zhongdao Wang, James T Kwok, Ping Luo, Huchuan Lu, and Zhenguo Li. Pixart- $\alpha$ : Fast training of diffusion transformer for photorealistic text-to-image synthesis. In *ICLR*, 2024.
- [15] Junying Chen, Zhenyang Cai, Pengcheng Chen, Shunian Chen, Ke Ji, Xidong Wang, Yunjin Yang, and Benyou Wang. Sharegpt-4o-image: Aligning multimodal models with gpt-4o-level image generation. *arXiv preprint arXiv:2506.18095*, 2025.

- [16] Li Chen, Mengyi Zhao, Yiheng Liu, Mingxu Ding, Yangyang Song, Shizun Wang, Xu Wang, Hao Yang, Jing Liu, Kang Du, et al. Photoverse: Tuning-free image customization with text-to-image diffusion models. *arXiv preprint arXiv:2309.05793*, 2023.
- [17] Liang Chen, Shuai Bai, Wenhao Chai, Weichu Xie, Haozhe Zhao, Leon Vinci, Junyang Lin, and Baobao Chang. Multimodal representation alignment for image generation: Text-image interleaved control is easier than you think. *arXiv preprint arXiv:2502.20172*, 2025.
- [18] Wenhui Chen, Hexiang Hu, Chitwan Saharia, and William W Cohen. Re-imagen: Retrieval-augmented text-to-image generator. *arXiv preprint arXiv:2209.14491*, 2022.
- [19] Xi Chen, Zhifei Zhang, He Zhang, Yuqian Zhou, Soo Ye Kim, Qing Liu, Yijun Li, Jianming Zhang, Nanxuan Zhao, Yilin Wang, et al. Unireal: Universal image generation and editing via learning real-world dynamics. In *Proceedings of the Computer Vision and Pattern Recognition Conference*, pages 12501–12511, 2025.
- [20] Xiaokang Chen, Chengyue Wu, Zhiyu Wu, Yiyang Ma, Xingchao Liu, Zizheng Pan, Wen Liu, Zhenda Xie, Xingkai Yu, Chong Ruan, and Ping Luo. Janus-pro: Unified multimodal understanding and generation with data and model scaling. *arXiv preprint arXiv:2501.17811*, 2025.
- [21] Xiaokang Chen, Zhiyu Wu, Xingchao Liu, Zizheng Pan, Wen Liu, Zhenda Xie, Xingkai Yu, and Chong Ruan. Janus-pro: Unified multimodal understanding and generation with data and model scaling. *arXiv preprint arXiv:2501.17811*, 2025.
- [22] Zhe Chen, Weiyun Wang, Yue Cao, Yangzhou Liu, Zhangwei Gao, Erfei Cui, Jinguo Zhu, Shenglong Ye, Hao Tian, Zhaoyang Liu, Lixin Gu, Xuehui Wang, Qingyun Li, Yimin Ren, Zixuan Chen, Jiapeng Luo, Jiahao Wang, Tan Jiang, Bo Wang, Conghui He, Botian Shi, Xingcheng Zhang, Han Lv, Yi Wang, Wenqi Shao, Pei Chu, Zhongying Tu, Tong He, Zhiyong Wu, Huipeng Deng, Jiaye Ge, Kai Chen, Kaipeng Zhang, Limin Wang, Min Dou, Lewei Lu, Xizhou Zhu, Tong Lu, Dahua Lin, Yu Qiao, Jifeng Dai, and Wenhui Wang. Expanding performance boundaries of open-source multimodal models with model, data, and test-time scaling. *arXiv preprint arXiv:2412.05271*, 2024.
- [23] Zhe Chen, Weiyun Wang, Hao Tian, Shenglong Ye, Zhangwei Gao, Erfei Cui, Wenwen Tong, Kongzhi Hu, Jiapeng Luo, Zheng Ma, et al. Internvl2: Better than the best—expanding performance boundaries of open-source multimodal models with the progressive scaling strategy, 2024. URL <https://internvl.github.io/blog/2024-07-02-InternVL-2-0>.
- [24] Guillaume Couairon, Jakob Verbeek, Holger Schwenk, and Matthieu Cord. Diffedit: Diffusion-based semantic image editing with mask guidance. *arXiv preprint arXiv:2210.11427*, 2022.
- [25] Google DeepMind. Gemini 2.0. <https://gemini.google.com/>, 2025.
- [26] Chaorui Deng, Deyao Zhu, Kunchang Li, Chenhui Gou, Feng Li, Zeyu Wang, Shu Zhong, Weihao Yu, Xiaonan Nie, Ziang Song, et al. Emerging properties in unified multimodal pretraining. *arXiv preprint arXiv:2505.14683*, 2025.
- [27] Patrick Esser, Sumith Kulal, Andreas Blattmann, Rahim Entezari, Jonas Müller, Harry Saini, Yam Levi, Dominik Lorenz, Axel Sauer, Frederic Boesel, et al. Scaling rectified flow transformers for high-resolution image synthesis. In *ICML*, 2024.
- [28] Patrick Esser, Sumith Kulal, Andreas Blattmann, Rahim Entezari, Jonas Müller, Harry Saini, Yam Levi, Dominik Lorenz, Axel Sauer, Frederic Boesel, et al. Scaling rectified flow transformers for high-resolution image synthesis. In *ICML*, 2024.
- [29] Tsu-Jui Fu, Yusu Qian, Chen Chen, Wenze Hu, Zhe Gan, and Yinfei Yang. Univg: A generalist diffusion model for unified image generation and editing. *arXiv preprint arXiv:2503.12652*, 2025.
- [30] Rinon Gal, Yuval Alaluf, Yuval Atzmon, Or Patashnik, Amit H Bermano, Gal Chechik, and Daniel Cohen-Or. An image is worth one word: Personalizing text-to-image generation using textual inversion. *arXiv preprint arXiv:2208.01618*, 2022.

[31] Yu Gao, Lixue Gong, Qiushan Guo, Xiaoxia Hou, Zhichao Lai, Fanshi Li, Liang Li, Xiaochen Lian, Chao Liao, Liyang Liu, et al. Seedream 3.0 technical report. *arXiv preprint arXiv:2504.11346*, 2025.

[32] Yuying Ge, Sijie Zhao, Chen Li, Yixiao Ge, and Ying Shan. Seed-data-edit technical report: A hybrid dataset for instructional image editing. *arXiv preprint arXiv:2405.04007*, 2024.

[33] Dhruba Ghosh, Hannaneh Hajishirzi, and Ludwig Schmidt. Geneval: An object-focused framework for evaluating text-to-image alignment. *Advances in Neural Information Processing Systems*, 36:52132–52152, 2023.

[34] Zinan Guo, Pengze Zhang, Yanze Wu, Chong Mou, Songtao Zhao, and Qian He. Musar: Exploring multi-subject customization from single-subject dataset via attention routing. *arXiv preprint arXiv:2505.02823*, 2025.

[35] Zhen Han, Zeyinzi Jiang, Yulin Pan, Jingfeng Zhang, Chaojie Mao, Chenwei Xie, Yu Liu, and Jingren Zhou. Ace: All-round creator and editor following instructions via diffusion transformer. *arXiv preprint arXiv:2410.00086*, 2024.

[36] Amir Hertz, Ron Mokady, Jay Tenenbaum, Kfir Aberman, Yael Pritch, and Daniel Cohen-Or. Prompt-to-prompt image editing with cross attention control. *arXiv preprint arXiv:2208.01626*, 2022.

[37] Jonathan Ho, Ajay Jain, and Pieter Abbeel. Denoising diffusion probabilistic models. In *NeurIPS*, 2020.

[38] Jonathan Ho, Chitwan Saharia, William Chan, David J Fleet, Mohammad Norouzi, and Tim Salimans. Cascaded diffusion models for high fidelity image generation. *Journal of Machine Learning Research*, 23(47):1–33, 2022.

[39] Edward J Hu, Yelong Shen, Phillip Wallis, Zeyuan Allen-Zhu, Yuanzhi Li, Shean Wang, Lu Wang, and Weizhu Chen. Lora: Low-rank adaptation of large language models. *arXiv:2106.09685*, 2021.

[40] Qihan Huang, Siming Fu, Jinlong Liu, Hao Jiang, Yipeng Yu, and Jie Song. Resolving multi-condition confusion for finetuning-free personalized image generation. *arXiv preprint arXiv:2409.17920*, 2024.

[41] Yuzhou Huang, Liangbin Xie, Xintao Wang, Ziyang Yuan, Xiaodong Cun, Yixiao Ge, Jiantao Zhou, Chao Dong, Rui Huang, Ruimao Zhang, et al. Smartedit: Exploring complex instruction-based image editing with multimodal large language models. In *Proceedings of the IEEE/CVF Conference on Computer Vision and Pattern Recognition*, pages 8362–8371, 2024.

[42] Mude Hui, Siwei Yang, Bingchen Zhao, Yichun Shi, Heng Wang, Peng Wang, Yuyin Zhou, and Cihang Xie. Hq-edit: A high-quality dataset for instruction-based image editing. *arXiv preprint arXiv:2404.09990*, 2024.

[43] Bahjat Kawar, Shiran Zada, Oran Lang, Omer Tov, Huiwen Chang, Tali Dekel, Inbar Mosseri, and Michal Irani. Imagic: Text-based real image editing with diffusion models. In *Proceedings of the IEEE/CVF conference on computer vision and pattern recognition*, pages 6007–6017, 2023.

[44] Alexander Kirillov, Eric Mintun, Nikhila Ravi, Hanzi Mao, Chloe Rolland, Laura Gustafson, Tete Xiao, Spencer Whitehead, Alexander C Berg, Wan-Yen Lo, et al. Segment anything. In *ICCV*, 2023.

[45] Maksim Kuprashevich, Grigorii Alekseenko, Irina Tolstykh, Georgii Fedorov, Bulat Suleimanov, Vladimir Dokholyan, and Aleksandr Gordeev. Nohumansrequired: Autonomous high-quality image editing triplet mining. Available at SSRN 5381374, 2025.

[46] Maksim Kuprashevich, Grigorii Alekseenko, Irina Tolstykh, Georgii Fedorov, Bulat Suleimanov, Vladimir Dokholyan, and Aleksandr Gordeev. Nohumansrequired: Autonomous high-quality image editing triplet mining. *arXiv preprint arXiv:2507.14119*, 2025.

[47] Black Forest Labs. Flux, 2024. URL <https://github.com/black-forest-labs/flux>.

[48] Black Forest Labs, Stephen Batifol, Andreas Blattmann, Frederic Boesel, Saksham Consul, Cyril Diagne, Tim Dockhorn, Jack English, Zion English, Patrick Esser, et al. Flux. 1 kontext: Flow matching for in-context image generation and editing in latent space. *arXiv preprint arXiv:2506.15742*, 2025.

[49] Dongxu Li, Junnan Li, and Steven Hoi. Blip-diffusion: Pre-trained subject representation for controllable text-to-image generation and editing. *Advances in Neural Information Processing Systems*, 36:30146–30166, 2023.

[50] Qingyun Li, Zhe Chen, Weiyun Wang, Wenhui Wang, Shenglong Ye, Zhenjiang Jin, Guanzhou Chen, Yinan He, Zhangwei Gao, Erfei Cui, et al. Omnicorpus: A unified multimodal corpus of 10 billion-level images interleaved with text. *arXiv preprint arXiv:2406.08418*, 2024.

[51] Yaowei Li, Yuxuan Bian, Xuan Ju, Zhaoyang Zhang, Junhao Zhuang, Ying Shan, Yuexian Zou, and Qiang Xu. Brushedit: All-in-one image inpainting and editing. *arXiv preprint arXiv:2412.10316*, 2024.

[52] Bin Lin, Zongjian Li, Xinhua Cheng, Yuwei Niu, Yang Ye, Xianyi He, Shenghai Yuan, Wangbo Yu, Shaodong Wang, Yunyang Ge, et al. Uniworld-v1: High-resolution semantic encoders for unified visual understanding and generation. *arXiv preprint arXiv:2506.03147*, 2025.

[53] Shilong Liu, Zhaoyang Zeng, Tianhe Ren, Feng Li, Hao Zhang, Jie Yang, Chun yue Li, Jianwei Yang, Hang Su, Jun-Juan Zhu, and Lei Zhang. Grounding dino: Marrying dino with grounded pre-training for open-set object detection. *arXiv:2303.05499*, 2023.

[54] Shiyu Liu, Yucheng Han, Peng Xing, Fukun Yin, Rui Wang, Wei Cheng, Jiaqi Liao, Yingming Wang, Honghao Fu, Chunrui Han, Guopeng Li, Yuang Peng, Quan Sun, Jingwei Wu, Yan Cai, Zheng Ge, Ranchen Ming, Lei Xia, Xianfang Zeng, Yibo Zhu, Binxing Jiao, Xiangyu Zhang, Gang Yu, and Daxin Jiang. Step1x-edit: A practical framework for general image editing. *arXiv preprint arXiv:2504.17761*, 2025.

[55] Shiyu Liu, Yucheng Han, Peng Xing, Fukun Yin, Rui Wang, Wei Cheng, Jiaqi Liao, Yingming Wang, Honghao Fu, Chunrui Han, et al. Step1x-edit: A practical framework for general image editing. *arXiv preprint arXiv:2504.17761*, 2025.

[56] Jian Ma, Junhao Liang, Chen Chen, and Haonan Lu. Subject-diffusion: Open domain personalized text-to-image generation without test-time fine-tuning. In *ACM SIGGRAPH 2024 Conference Papers*, pages 1–12, 2024.

[57] Yiyang Ma, Xingchao Liu, Xiaokang Chen, Wen Liu, Chengyue Wu, Zhiyu Wu, Zizheng Pan, Zhenda Xie, Haowei Zhang, Xingkai Yu, Liang Zhao, Yisong Wang, Jiaying Liu, and Chong Ruan. Janusflow: Harmonizing autoregression and rectified flow for unified multimodal understanding and generation. *arXiv preprint arXiv:2411.07975*, 2024.

[58] Yiyang Ma, Xingchao Liu, Xiaokang Chen, Wen Liu, Chengyue Wu, Zhiyu Wu, Zizheng Pan, Zhenda Xie, Haowei Zhang, Xingkai Yu, et al. Janusflow: Harmonizing autoregression and rectified flow for unified multimodal understanding and generation. In *Proceedings of the Computer Vision and Pattern Recognition Conference*, pages 7739–7751, 2025.

[59] Chaojie Mao, Jingfeng Zhang, Yulin Pan, Zeyinzi Jiang, Zhen Han, Yu Liu, and Jingren Zhou. Ace++: Instruction-based image creation and editing via context-aware content filling. *arXiv preprint arXiv:2501.02487*, 2025.

[60] Chenlin Meng, Yutong He, Yang Song, Jiaming Song, Jiajun Wu, Jun-Yan Zhu, and Stefano Ermon. Sdedit: Guided image synthesis and editing with stochastic differential equations. *arXiv preprint arXiv:2108.01073*, 2021.

[61] Ron Mokady, Amir Hertz, Kfir Aberman, Yael Pritch, and Daniel Cohen-Or. Null-text inversion for editing real images using guided diffusion models. In *Proceedings of the IEEE/CVF conference on computer vision and pattern recognition*, pages 6038–6047, 2023.

[62] Alexander Quinn Nichol and Prafulla Dhariwal. Improved denoising diffusion probabilistic models. In *ICML*, 2021.

[63] OpenAI. Gpt-4v(ision) system card, 2023. URL <https://openai.com/research/gpt-4v-system-card>.

[64] OpenAI. Introducing 4o image generation, March 2025. URL <https://openai.com/index/introducing-4o-image-generation/>. Accessed: 2025-05-09.

[65] OpenAI. Gpt-image-1, 2025. URL <https://openai.com/index/introducing-4o-image-generation/>.

[66] Xichen Pan, Satya Narayan Shukla, Aashu Singh, Zhuokai Zhao, Shlok Kumar Mishra, Jialiang Wang, Zhiyang Xu, Juhai Chen, Kunpeng Li, Felix Juefei-Xu, Ji Hou, and Saining Xie. Transfer between modalities with metaqueries. *arXiv preprint arXiv:2504.06256*, 2025.

[67] Gaurav Parmar, Krishna Kumar Singh, Richard Zhang, Yijun Li, Jingwan Lu, and Jun-Yan Zhu. Zero-shot image-to-image translation. In *ACM SIGGRAPH 2023 conference proceedings*, pages 1–11, 2023.

[68] Dustin Podell, Zion English, Kyle Lacey, Andreas Blattmann, Tim Dockhorn, Jonas Müller, Joe Penna, and Robin Rombach. Sdxl: Improving latent diffusion models for high-resolution image synthesis. In *ICLR*, 2024.

[69] Qi Qin, Le Zhuo, Yi Xin, Ruoyi Du, Zhen Li, Bin Fu, Yiting Lu, Jiakang Yuan, Xinyue Li, Dongyang Liu, et al. Lumina-image 2.0: A unified and efficient image generative framework. *arXiv preprint arXiv:2503.21758*, 2025.

[70] Nataniel Ruiz, Yuanzhen Li, Varun Jampani, Yael Pritch, Michael Rubinstein, and Kfir Aberman. Dreambooth: Fine tuning text-to-image diffusion models for subject-driven generation. In *CVPR*, pages 22500–22510, 2023.

[71] Weijia Shi, Xiaochuang Han, Chunting Zhou, Weixin Liang, Xi Victoria Lin, Luke Zettlemoyer, and Lili Yu. Llamafusion: Adapting pretrained language models for multimodal generation. *arXiv preprint arXiv:2412.15188*, 2024.

[72] Wensong Song, Hong Jiang, Zongxing Yang, Ruijie Quan, and Yi Yang. Insert anything: Image insertion via in-context editing in dit. *arXiv preprint arXiv:2504.15009*, 2025.

[73] Jianlin Su, Murtadha Ahmed, Yu Lu, Shengfeng Pan, Wen Bo, and Yunfeng Liu. Roformer: Enhanced transformer with rotary position embedding. *Neurocomputing*, 568:127063, 2024.

[74] Zhenxiong Tan, Songhua Liu, Xingyi Yang, Qiaochu Xue, and Xinchao Wang. Ominicontrol: Minimal and universal control for diffusion transformer. *arXiv preprint arXiv:2411.15098*, 2024.

[75] Chameleon Team. Chameleon: Mixed-modal early-fusion foundation models. *arXiv preprint arXiv:2405.09818*, 2024.

[76] Shengbang Tong, David Fan, Jiachen Zhu, Yunyang Xiong, Xinlei Chen, Koustuv Sinha, Michael Rabbat, Yann LeCun, Saining Xie, and Zhuang Liu. Metamorph: Multimodal understanding and generation via instruction tuning. *arXiv preprint arXiv:2412.14164*, 2024.

[77] Michael Tschannen, Alexey Gritsenko, Xiao Wang, Muhammad Ferjad Naeem, Ibrahim Alabdulmohsin, Nikhil Parthasarathy, Talfan Evans, Lucas Beyer, Ye Xia, Basil Mustafa, et al. Siglip 2: Multilingual vision-language encoders with improved semantic understanding, localization, and dense features. *arXiv preprint arXiv:2502.14786*, 2025.

[78] Bram Wallace, Akash Gokul, and Nikhil Naik. Edict: Exact diffusion inversion via coupled transformations. In *Proceedings of the IEEE/CVF Conference on Computer Vision and Pattern Recognition*, pages 22532–22541, 2023.

[79] Jiangshan Wang, Junfu Pu, Zhongang Qi, Jiayi Guo, Yue Ma, Nisha Huang, Yuxin Chen, Xiu Li, and Ying Shan. Taming rectified flow for inversion and editing. *arXiv preprint arXiv:2411.04746*, 2024.

[80] Peng Wang, Shuai Bai, Sinan Tan, Shijie Wang, Zhihao Fan, Jinze Bai, Keqin Chen, Xuejing Liu, Jialin Wang, Wenbin Ge, Yang Fan, Kai Dang, Mengfei Du, Xuancheng Ren, Rui Men, Dayiheng Liu, Chang Zhou, Jingren Zhou, and Junyang Lin. Qwen2-vl: Enhancing vision-language model’s perception of the world at any resolution. *arXiv:2409.12191*, 2024.

[81] Peng Wang, Shuai Bai, Sinan Tan, Shijie Wang, Zhihao Fan, Jinze Bai, Keqin Chen, Xuejing Liu, Jialin Wang, Wenbin Ge, Yang Fan, Kai Dang, Mengfei Du, Xuancheng Ren, Rui Men, Dayiheng Liu, Chang Zhou, Jingren Zhou, and Junyang Lin. Qwen2-vl: Enhancing vision-language model’s perception of the world at any resolution. *arXiv preprint arXiv:2409.12191*, 2024.

[82] Peng Wang, Yichun Shi, Xiaochen Lian, Zhonghua Zhai, Xin Xia, Xuefeng Xiao, Weilin Huang, and Jianchao Yang. Seededit 3.0: Fast and high-quality generative image editing. *arXiv preprint arXiv:2506.05083*, 2025.

[83] Qixun Wang, Xu Bai, Haofan Wang, Zekui Qin, Anthony Chen, Huaxia Li, Xu Tang, and Yao Hu. Instantid: Zero-shot identity-preserving generation in seconds. *arXiv preprint arXiv:2401.07519*, 2024.

[84] Xierui Wang, Siming Fu, Qihan Huang, Wanggui He, and Hao Jiang. MS-diffusion: Multi-subject zero-shot image personalization with layout guidance. In *ICLR*, 2025. URL <https://openreview.net/forum?id=PJqP0wyQek>.

[85] Xinlong Wang, Xiaosong Zhang, Zhengxiong Luo, Quan Sun, Yufeng Cui, Jinsheng Wang, Fan Zhang, Yueze Wang, Zhen Li, Qiying Yu, et al. Emu3: Next-token prediction is all you need. *arXiv preprint arXiv:2409.18869*, 2024.

[86] Xinlong Wang, Xiaosong Zhang, Zhengxiong Luo, Quan Sun, Yufeng Cui, Jinsheng Wang, Fan Zhang, Yueze Wang, Zhen Li, Qiying Yu, et al. Emu3: Next-token prediction is all you need. *arXiv preprint arXiv:2409.18869*, 2024.

[87] Cong Wei, Zheyang Xiong, Weiming Ren, Xeron Du, Ge Zhang, and Wenhui Chen. Omnidit: Building image editing generalist models through specialist supervision. In *ICLR*, 2024.

[88] Yuxiang Wei, Yabo Zhang, Zhilong Ji, Jinfeng Bai, Lei Zhang, and Wangmeng Zuo. Elite: Encoding visual concepts into textual embeddings for customized text-to-image generation. In *CVPR*, pages 15943–15953, 2023.

[89] Peebles William and Saining Xie. Scalable diffusion models with transformers. In *ICCV*, 2023.

[90] Chenfei Wu, Jiahao Li, Jingren Zhou, Junyang Lin, Kaiyuan Gao, Kun Yan, Shengming Yin, Shuai Bai, Xiao Xu, Yilei Chen, Yuxiang Chen, Zecheng Tang, Zekai Zhang, Zhengyi Wang, An Yang, Bowen Yu, Chen Cheng, Dayiheng Liu, Deqing Li, Hang Zhang, Hao Meng, Hu Wei, Jingyuan Ni, Kai Chen, Kuan Cao, Liang Peng, Lin Qu, Minggang Wu, Peng Wang, Shuting Yu, Tingkun Wen, Wensen Feng, Xiaoxiao Xu, Yi Wang, Yichang Zhang, Yongqiang Zhu, Yujia Wu, Yuxuan Cai, and Zenan Liu. Qwen-image technical report, 2025. URL <https://arxiv.org/abs/2508.02324>.

[91] Chengyue Wu, Xiaokang Chen, Zhiyu Wu, Yiyang Ma, Xingchao Liu, Zizheng Pan, Wen Liu, Zhenda Xie, Xingkai Yu, Chong Ruan, and Ping Luo. Janus: Decoupling visual encoding for unified multimodal understanding and generation. *arXiv preprint arXiv:2410.13848*, 2024.

[92] Chenyuan Wu, Pengfei Zheng, Ruiran Yan, Shitao Xiao, Xin Luo, Yueze Wang, Wanli Li, Xiyuan Jiang, Yixin Liu, Junjie Zhou, et al. Omnigen2: Exploration to advanced multimodal generation. *arXiv preprint arXiv:2506.18871*, 2025.

[93] Shaojin Wu, Mengqi Huang, Wenxu Wu, Yufeng Cheng, Fei Ding, and Qian He. Less-to-more generalization: Unlocking more controllability by in-context generation. *arXiv preprint arXiv:2504.02160*, 2025.

[94] Shitao Xiao, Yueze Wang, Junjie Zhou, Huaying Yuan, Xingrun Xing, Ruiran Yan, Chaofan Li, Shuting Wang, Tiejun Huang, and Zheng Liu. Omnigen: Unified image generation. *arXiv preprint arXiv:2409.11340*, 2024.

[95] Shitao Xiao, Yueze Wang, Junjie Zhou, Huaying Yuan, Xingrun Xing, Ruiran Yan, Chaofan Li, Shuteng Wang, Tiejun Huang, and Zheng Liu. Omnigen: Unified image generation. In *Proceedings of the Computer Vision and Pattern Recognition Conference*, pages 13294–13304, 2025.

[96] Jinheng Xie, Weijia Mao, Zechen Bai, David Junhao Zhang, Weihao Wang, Kevin Qinghong Lin, Yuchao Gu, Zhijie Chen, Zhenheng Yang, and Mike Zheng Shou. Show-o: One single transformer to unify multimodal understanding and generation. *arXiv preprint arXiv:2408.12528*, 2024.

[97] Jinheng Xie, Zhenheng Yang, and Mike Zheng Shou. Show-o2: Improved native unified multimodal models. *arXiv preprint arXiv:2506.15564*, 2025.

[98] Yingjing Xu, Jie Kong, Jiazhi Wang, Xiao Pan, Bo Lin, and Qiang Liu. Insightsedit: Towards better instruction following for image editing. In *Proceedings of the Computer Vision and Pattern Recognition Conference*, pages 2694–2703, 2025.

[99] Huanjin Yao, Jiaxing Huang, Wenhao Wu, Jingyi Zhang, Yibo Wang, Shunyu Liu, Yingjie Wang, Yuxin Song, Haocheng Feng, Li Shen, et al. Mulberry: Empowering mllm with o1-like reasoning and reflection via collective monte carlo tree search. *arXiv preprint arXiv:2412.18319*, 2024.

[100] Huanjin Yao, Wenhao Wu, Taojiannan Yang, YuXin Song, Mengxi Zhang, Haocheng Feng, Yifan Sun, Zhiheng Li, Wanli Ouyang, and Jingdong Wang. Dense connector for mllms. *Advances in Neural Information Processing Systems*, 37:33108–33140, 2024.

[101] Hu Ye, Jun Zhang, Sibo Liu, Xiao Han, and Wei Yang. Ip-adapter: Text compatible image prompt adapter for text-to-image diffusion models. *arXiv preprint arXiv:2308.06721*, 2023.

[102] Yang Ye, Xianyi He, Zongjian Li, Bin Lin, Shenghai Yuan, Zhiyuan Yan, Bohan Hou, and Li Yuan. Imgedit: A unified image editing dataset and benchmark. *arXiv preprint arXiv:2505.20275*, 2025.

[103] Qifan Yu, Wei Chow, Zhongqi Yue, Kaihang Pan, Yang Wu, Xiaoyang Wan, Juncheng Li, Siliang Tang, Hanwang Zhang, and Yuetong Zhuang. Anyedit: Mastering unified high-quality image editing for any idea. In *Proceedings of the Computer Vision and Pattern Recognition Conference*, pages 26125–26135, 2025.

[104] Kai Zhang, Lingbo Mo, Wenhui Chen, Huan Sun, and Yu Su. Magicbrush: A manually annotated dataset for instruction-guided image editing. *Advances in Neural Information Processing Systems*, 36:31428–31449, 2023.

[105] Shu Zhang, Xinyi Yang, Yihao Feng, Can Qin, Chia-Chih Chen, Ning Yu, Zeyuan Chen, Huan Wang, Silvio Savarese, Stefano Ermon, et al. Hive: Harnessing human feedback for instructional visual editing. In *Proceedings of the IEEE/CVF Conference on Computer Vision and Pattern Recognition*, pages 9026–9036, 2024.

[106] Zechuan Zhang, Ji Xie, Yu Lu, Zongxin Yang, and Yi Yang. In-context edit: Enabling instructional image editing with in-context generation in large scale diffusion transformer. *arXiv preprint arXiv:2504.20690*, 2025.

[107] Zechuan Zhang, Ji Xie, Yu Lu, Zongxin Yang, and Yi Yang. In-context edit: Enabling instructional image editing with in-context generation in large scale diffusion transformer. *arXiv preprint arXiv:2504.20690*, 2025.

[108] Chuyang Zhao, YuXin Song, Junru Chen, Kang Rong, Haocheng Feng, Gang Zhang, Shufan Ji, Jingdong Wang, Errui Ding, and Yifan Sun. Octopus: A multi-modal llm with parallel recognition and sequential understanding. *Advances in Neural Information Processing Systems*, 37:90009–90029, 2024.

[109] Haozhe Zhao, Xiaojian Shawn Ma, Liang Chen, Shuzheng Si, Ruijie Wu, Kaikai An, Peiyu Yu, Minjia Zhang, Qing Li, and Baobao Chang. Ultraedit: Instruction-based fine-grained image editing at scale. *Advances in Neural Information Processing Systems*, 37:3058–3093, 2024.

- [110] Chunting Zhou, Lili Yu, Arun Babu, Kushal Tirumala, Michihiro Yasunaga, Leonid Shamis, Jacob Kahn, Xuezhe Ma, Luke Zettlemoyer, and Omer Levy. Transfusion: Predict the next token and diffuse images with one multi-modal model. *arXiv preprint arxiv:2408.11039*, 2024.
- [111] Wanrong Zhu, Jack Hessel, Anas Awadalla, Samir Yitzhak Gadre, Jesse Dodge, Alex Fang, Youngjae Yu, Ludwig Schmidt, William Yang Wang, and Yejin Choi. Multimodal c4: An open, billion-scale corpus of images interleaved with text. *Advances in Neural Information Processing Systems*, 36:8958–8974, 2023.